Observation of Self-Amplified Spontaneous-Emission-Induced Electron-Beam Microbunching Using Coherent Transition Radiation

A. Tremaine, J. B. Rosenzweig, S. Anderson, P. Frigola, M. Hogan, A. Murokh, and C. Pellegrini
Department of Physics and Astronomy, UCLA, 405 Hilgard Avenue, Los Angeles, California 90095-1547

D. C. Nguyen and R. L. Sheffield
Los Alamos National Laboratory, Los Alamos, New Mexico 87545
(Received 9 July 1998)

We report the measurement of electron-beam microbunching at the exit of a self-amplified spontaneous-emission free-electron laser (SASE FEL), by observation of coherent transition radiation (CTR). The CTR was found to have an angular spectrum much narrower than spontaneous transition radiation and a narrow-band frequency spectrum. The central frequency of the fundamental CTR spectrum is found to differ slightly from that of the SASE, a finding in disagreement with previously invoked CTR theory. The CTR measurement establishes the uniformity of microbunching in the transverse dimension, indicating the SASE FEL operates in a dominant transverse mode. [S0031-9007(98)08027-2]

PACS numbers: 41.60.Cr, 41.60.Ap

Charged particle beams with microbunch structure, the periodic modulation of the beam longitudinal profile, are now present in a variety of experimental scenarios, e.g., free-electron lasers (FELs) [1], their inverse (IFELs) [2], and advanced accelerators based on laser excitation of plasmas and structures [3]. In the present investigation, we focus on the microbunching that develops as a result of the self-amplified spontaneous emission FEL (SASE FEL) process [4]. This microbunching, which occurs at the wavelength of the FEL radiation, is central to the FEL gain process, as such a distribution produces radiation coherently, giving rise to exponential gain.

The creation of ever shorter time structures in particle beams has pushed the methods of longitudinal beam diagnosis past the reach of time domain methods, such as streak cameras [5] and rf sweeping [6], into the frequency domain. Methods using coherent transition radiation (CTR) have found wide use in diagnosing macrobunches at the picosecond level [7,8]. CTR-based methods rely on the fact that the spectrum of coherent radiation emitted by the beam as it passes a transition radiation foil is essentially the Fourier transform of the longitudinal beam distribution. The transverse distribution is usually unimportant in this case, because the bunch width is typically much smaller than its length. This is not the case for microbunching-induced CTR, as the wavelength of the radiation is smaller than the bunch width [9].

The traditional analysis of CTR begins by writing the differential radiation spectrum due to multiparticle coherence effects as a function proportional to the single particle spectrum [8],

$$\frac{d^2U}{d\omega\, d\Omega} \cong N_b^2 F_L(\omega) F_T(\omega,\theta)\chi(\theta)\, \frac{d^2U}{d\omega\, d\Omega}\bigg|_{1\, e^-}, \tag{1}$$

where N_B is the bunch population and $F_L(\omega)$ and $F_T(\omega,\theta)$ are the Fourier transform square amplitudes of the longitudinal (time) and transverse beam profiles, respectively. The factor $\chi(\theta)$ is due to the finite divergence of the beam and is usually taken to be close to unity. For narrow band transition radiation, however, this factor is not ignorable, as we shall see below.

The case of a microbunched beam produced, e.g., in an FEL or IFEL, has been worked out in detail in Ref. [9]. Here we need to extend the previous results to account for asymmetries in the beam transverse distribution. The microbunched beam distribution is therefore taken to be

$$f(r,z) = \frac{N_b}{(2\pi)^{3/2}\sigma_x\sigma_y\sigma_z}\exp\left(-\frac{x^2}{2\sigma_x^2} - \frac{y^2}{2\sigma_y^2} - \frac{z^2}{2\sigma_z^2}\right) \times \left[1 + \sum_{n=1}^{\infty} b_n \sin(nk_r z)\right], \tag{2}$$

where k_r is the radiation and, therefore, beam modulation wave number. Because the beam has Fourier components at k_r and its harmonics, an analysis following the methods of Ref. [9] predicts that the wave spectrum of CTR is localized in peaks near these frequencies, with an angular spectrum of photon number at each peak $k = nk_r$ of

$$\frac{dN_\gamma}{d\theta} \cong \frac{\alpha(N_b b_n)^2}{4\sqrt{\pi}\, nk_r\sigma_z}\, \frac{\sin^3(\theta)}{[1-\beta\cos(\theta)]^2}\exp\{-[nk_r\sin(\theta)]^2[\sigma_x^2\sin^2(\phi) + \sigma_y^2\cos^2(\phi)]\}\,\chi(\theta), \tag{3}$$

where θ and ϕ are the polar and azimuthal angles with respect to the beam axis, respectively, and $\alpha \cong \frac{1}{137}$. Several

 0031-9007/98/81(26)/5816(4)$15.00

predictions can be deduced from Eq. (3): First, the number of photons scales as the square of the number of radiators N_b^2. Also, the angular spectrum is narrowed considerably (when, as in the cases of present interest, $nk\sigma_{x,y}/\gamma > 1$) by the transverse geometric factor, which expresses the diffraction-limited nature (as opposed to the natural transition radiation angular distribution) of the coherent radiation, which for an axisymmetric beam of size σ gives a diffraction angle of $\theta_d = (\sqrt{2}\,nk_r\sigma)^{-1}$. This narrowing is a signature of coherence for the microbunched case, where the beam has a relatively uniform distribution many wavelengths across. If the beam distribution has notable transverse dependence, the coherent radiation may be found in a more complicated pattern at larger angles.

If we ignore the divergence factor $[\chi(\theta) \approx 1]$ and perform the angular integration, we obtain a predicted number of emitted photons at each harmonic (for forward CTR, normal beam incidence),

$$N_\gamma \approx \frac{\alpha(N_b b_n)^2}{4\sqrt{\pi}\,k_r\sigma_z}\left(\frac{\gamma}{nk_r}\right)^4\left(\frac{\sigma_x^2 + \sigma_y^2}{\sigma_x^3\sigma_y^3}\right), \qquad (4)$$

which illustrates also the sensitive dependence of the CTR on beam dimensions. CTR is enhanced when the beam is dense (N_b is large; σ's are small), and there are many radiating electrons bunched within a cubic half wavelength (b_n not small).

A measurement of some of these effects has been carried out at BNL [10], where a 0.3 nC electron beam was strongly bunched by the IFEL interaction with a 10.6 μm laser. The electron beam was not well focused at the foil (transverse beam size 0.6 by 5.5 mm), however, and so the CTR intensity was weak. To measure CTR in this experiment, a large signal at the IFEL fundamental had to be suppressed, by looking at the forward radiation behind the opaque $d = 63$ μm Cu foil. The primary result of this measurement was demonstration of a quadratic dependence of N_γ on N_b. Also, high-pass filters were used to establish CTR at or above the fourth IFEL harmonic. It is important that both effects have been previously established, as neither is easily seen in a SASE FEL experiment. The dependence $N_\gamma \sim N_b^2$ is not observable in a SASE experiment as the bunching factors b_n are gain and thus N_b dependent. In addition, the $b_n \propto b_1^n$ are negligibly small unless the FEL is near saturation, which is not the case despite the high gain achieved in this experiment.

Because of the signal level, asymmetric beam, and calibration factors, the overall photon number was not given, nor compared to theoretical predictions for the BNL results. This exercise would have been problematic for the BNL case in any event, as scattering effects in the foil served to strongly suppress CTR production. Additionally, critical predictions of the microbunch CTR theory were not observed—the narrow-band frequency spectrum centered near the fundamental IFEL frequency and/or its harmonics and the narrowing of the angular spectrum to the diffraction limit. Both of these attributes taken together indicate microbunching structure, meaning periodic longitudinal organization of the electrons. The BNL results indicate the presence of high frequency components but do not strictly imply that the beam is organized into microbunches. In order to employ CTR as a method for diagnosing microbunching, all relevant aspects of the theory must be explored. The present measurements verify much of the theoretical model and give some insight into the microbunching process in a high-gain SASE FEL.

Our experiments were performed at the AFEL facility at Los Alamos National Laboratory, a 1300 MHz rf photoinjector which produces a 100-bunch train of low-emittance, high current electron bunches. The experimental setup is shown in Fig. 1, and the beam parameters relevant to this experiment, measured using the methods described in Ref. [11], are given in Table I. The undulator used was the 2 m UCLA/Kurchatov [11] device employed in recent high-gain SASE FEL experiments; its parameters are also displayed in Table I. The 6 μm thick Al CTR foil was mounted on an insertable actuator normal to the beam line, 1 cm after the undulator exit, in a large opaque stop, to eliminate all FEL radiation when the foil is inserted. This placement of the foil allowed us to collect FEL and CTR radiation alternatively in the same optical beam line. In addition, the beam defocuses transversely in 21 cm, and space charge effects are predicted to debunch the beam in roughly 50 cm from the end of the undulator [12]. These effects are avoided in our geometry. The optical beam line was set so that only diffraction-limited coherent radiation passes the acceptance angle $\theta_{\rm acc} \approx 12$ mrad, be collected, and focused into the detector. The incoherent TR, however, with its angular peak at $\theta_{\rm inc} \approx \gamma^{-1} = 29$ mrad, is collected with only a few percent efficiency. The detector provides an equilibrium output signal level proportional to the radiated energy per electron pulse, with the proportionality constant obtained from a calibrated laser power meter.

The conditions of high SASE FEL gain with a 1.5 nC beam seen in Ref. [11] were reestablished for this experiment. The performance of the FEL was optimized by setting the beam focus to the matched condition at the undulator entrance and fine-tuning the rf phase of the photoinjector. This procedure gave highest SASE output at relatively low injection phase, which corresponds to higher dynamical compression of the electron bunch, and thus higher peak current, FEL gain, and microbunching effect. After insertion of the foil, however, in addition to incremental changes in solenoid focusing, it was found that a small adjustment (2°–3°) of the rf phase was necessary to maximize in the CTR signal, as shown in Fig. 2. As the rf accelerating wave provides phase dependent focusing [13], this adjustment (which has a negligible effect on the final energy of the beam) serves to minimize the beam size attainable at the foil, thus optimizing the CTR production [cf. Eq. (4)]. The SASE signal is less sensitive to beam focusability, however, as the gain in this

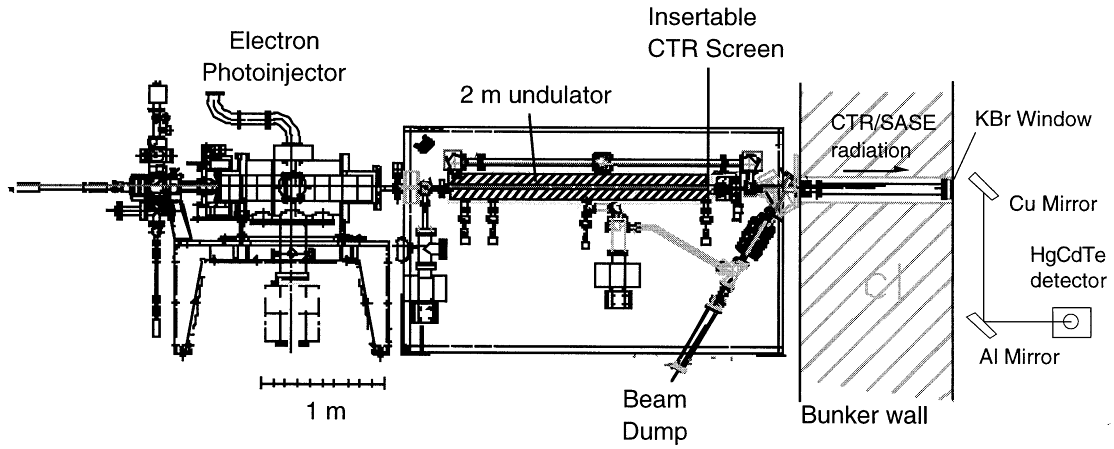

FIG. 1. Electron injector, undulator, and CTR/SASE optical beam line at LANL AFEL facility.

experiment is dominated by diffraction, which is mitigated with larger $\sigma_{x,y}$ [14]. The peak regions of the SASE and CTR signals as a function of rf phase overlap, as they must, because the CTR is dependent on the SASE-induced bunching. In our case, using the analysis of Ref. [11], the measured gain was near 10^5. The bunching predicted for these conditions by the 3D FEL simulation code GINGER, for a range of parameters corresponding to experimental uncertainties, was $b_1 = 0.008\text{–}0.01$, with negligible bunching at the higher harmonics.

Before discussing the data further, we remark that initial CTR measurements were attempted with a 50 μm Al foil, with the result that the CTR signal was weaker than expected, leading us to examine the effects of foil scattering. For an uncorrelated Gaussian phase space distribution typical of a scattered beam, a formalism has been developed [8] to evaluate $\chi(\theta)$. Several results of this analysis can be described. First, $\chi(\theta)$ is near unity for small angles when the angular spread of the incoherent radiation is large compared to the rms beam divergence, $\sigma' \cong \theta_{\text{scat}} \ll \gamma^{-1}$. If this condition is violated, $\chi(\theta)$ diminishes rapidly. After substitution of $\chi(\theta)$ into Eq. (3) and integrating, we can define a factor $\eta(\gamma\sigma')$ (keeping all other parameters constant) which indicates the degree of suppression of the CTR signal due to beam divergence. Note that since the scattering angle $\theta_{\text{scat}} \propto \gamma^{-1}d^{1/2}$, η is independent of γ and is a function only of foil material and thickness d. For our 50 μm Al foil, where $\theta_{\text{scat}} \approx \gamma^{-1}$, $\eta \cong 0.11$, and for the highly scattered BNL case $\eta \cong 5 \times 10^{-3}$. In order to avoid this effect, we need $\theta_{\text{scat}} \ll \gamma^{-1}$, which was achieved by using the 6 μm Al foil. Integrating Eq. (3), and multiplying by the factor $\eta = 0.61$ for our case yields a photon number, for the range of GINGER-predicted b_1 and other beam parameters given in Table I of $N_\gamma = (2.8\text{–}4.4) \times 10^8$. The measured photon number per pulse at the peak given in Fig. 2, obtained by calibrating the HgCdTe detector with a laser power meter, is $N_\gamma = 3.5 \times 10^8$. The theory, simulation, and experiment thus agree to within experimental and simulational uncertainty.

TABLE I. Beam and undulator parameters for CTR microbunching experiment.

Beam energy	E	17.5 MeV
Peak current	I	140 A
Charge/bunch	Q	1.5 nC
Bunch length (FWHM)	τ	11 psec
Energy spread	$\Delta\gamma/\gamma$	0.5%
Wiggler period	λW	2 cm
On-axis field	B_0	7.4 kG
FEL wavelength	λ	13 μm
FEL parameter	ρ	0.008
rms beam sizes	σ_x, σ_y	210, 160 μm

Having established an optimization procedure for both SASE and CTR, we then undertook a spectral study of both signals by use of a Jerrell Ash monochromator. To maximize the signal through the monochromator, its input collimating slits were removed, which resulted in a measured intrinsic resolution of 0.177 μm. The SASE and CTR spectra thus obtained (with the SASE attenuated by a factor of 3 and the CTR multiplied by 10 to

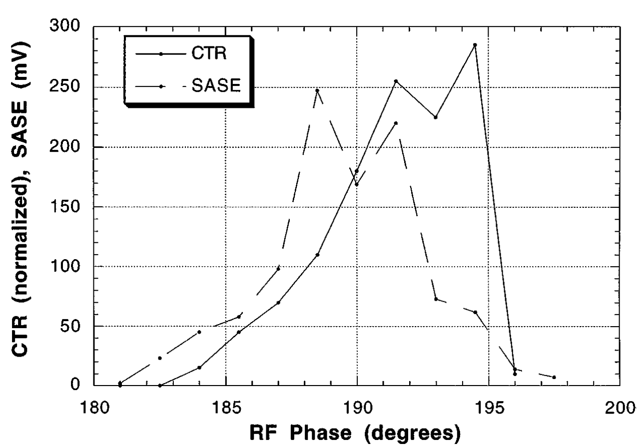

FIG. 2. SASE and CTR signals as a function of rf phase, with CTR scaled to SASE amplitude.

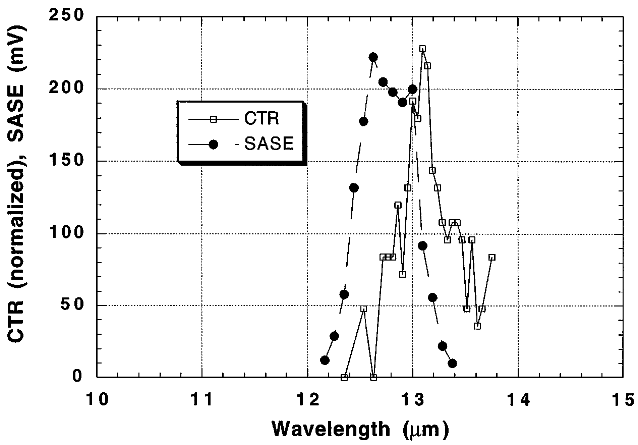

FIG. 3. SASE and CTR signals as a function of wavelength, with CTR scaled to SASE amplitude.

give similar scale), are shown in Fig. 3. Both the CTR and SASE signals are localized near the same wavelength, with a small difference in the distribution centers. This discrepancy points to a subtle error in the standard analysis of CTR [8,9]. Because the radiation components are summed by considering a temporal "snapshot" of the beam distribution [8], the off-axis Doppler shifting of the radiation, which is not created "at rest" by the foil, but over a radiation formation length [15] by the relativistic electrons, is not obtained. Within this region, the initially radiated energy can interact with the bunched beam to absorb and re-emit photons, thus rearranging the wavelength spectrum. Initial analysis of this effect indicates that it tends to shift the wavelength spectrum, as in the FEL, towards $\lambda \rightarrow \lambda[1 + (\gamma\theta)^2]$. While the SASE radiation is peaked at $\theta = 0$, the CTR is peaked off axis, which leads to a shift in the centroid of CTR wavelength with respect of SASE by $\Delta\lambda/\lambda \cong (\gamma/2k_r\sigma)^2 \cong 3.8\%$; the observed shift is 3.3%.

In conclusion, we have demonstrated two critical aspects of the microbunching-induced coherent transition radiation—the narrowing of the angular spectrum and the formation of line structure in the wavelength spectrum. These observations have verified some aspects of microbunching-induced CTR theoretical analysis but challenged others. In particular, this analysis must be redone employing a model where the beam interacts with the radiation over a formation length, as opposed to the instantaneous radiation model presently used [8,9]. Also, to have a well understood diagnostic, which produces the expected level of coherence, one must minimize the beam divergence induced by the CTR foil. It should be emphasized that this diagnostic method is important not only for FEL experiments but for short wavelength advanced accelerator experiments, such as the plasma accelerators [16], plasma-based injectors [17], and direct laser acceleration [3].

It is equally useful to view the current experiments from the FEL physics view point, as these measurements were performed at a SASE FEL exit, verifying the crucial role that microbunching plays in the gain process. The narrow angular spread of the CTR signal indicates that the microbunching is fairly uniform in the transverse dimension; otherwise, the CTR signal would have a less localized angular spectrum. This information indicates that the FEL is running with a dominant transverse mode and verifies the microbunching expected from the SASE process. Also, the agreement of measured and predicted photon number, using the microbunching given by simulations, is especially encouraging, as it provides an independent check on the code predictions. The CTR microbunching method will be even more useful in next generation SASE FEL experiments, in which the FEL should saturate. In this case the signal will be larger, not only on the fundamental radiation wavelength, but on the harmonics as well. The large signal levels will allow closer investigation of off-axis Doppler shift effects. The added information from harmonics should permit a more detailed reconstruction of the beam's microbunch distribution.

This work was supported by U.S. Department of Energy Grant No. DE-FG03-93ER0796 and Alfred P. Sloan Foundation Grant No. BR-3225.

[1] R. Bonifacio, C. Pellegrini, and L. Narducci, Opt. Commun. **50**, 373 (1984).
[2] A. Van Steenburgen *et al.*, Phys. Rev. Lett. **80**, 289 (1998).
[3] J. Rosenzweig *et al.*, Phys. Rev. Lett. **74**, 2467 (1995).
[4] R. Tatchyn *et al.*, Nucl. Instrum. Methods Phys. Res., Sect. A **375**, 274 (1996); C. Pellegrini *et al.*, Nucl. Instrum. Methods Phys. Res., Sect. A **331**, 223 (1993); J. Rossbach *et al.*, Nucl. Instrum. Methods Phys. Res., Sect. A **375**, 269 (1997).
[5] J. Gardelle *et al.*, Phys. Rev. Lett. **76**, 4532 (1996).
[6] B. Carlsten and S. J. Russell, Phys. Rev. E **53**, R2072 (1996).
[7] U. Happek, A. J. Sievers, and E. B. Blum, Phys. Rev. Lett. **67**, 2962 (1991); A. Murokh *et al.*, Nucl. Instrum. Methods Phys. Res., Sect. A (to be published).
[8] Yukio Shibata *et al.*, Phys. Rev. E **50**, 1479 (1994).
[9] J. B. Rosenzweig, G. Travish, and A. Tremaine, Nucl. Instrum. Methods Phys. Res., Sect. A **365**, 255 (1995).
[10] Y. Liu *et al.*, Phys. Rev. Lett. **80**, 4418 (1998); Y. Liu, Ph.D. thesis, UCLA Department of Physics and Astronomy, 1997.
[11] M. Hogan *et al.*, Phys. Rev. Lett. **81**, 4867 (1998).
[12] J. Rosenzweig *et al.*, Nucl. Instrum. Methods Phys. Res., Sect. A **393**, 376 (1997).
[13] S. Reiche *et al.*, Phys. Rev. E **56**, 3572 (1997); J. Rosenzweig and L. Serafini, Phys. Rev. E **49**, 1499 (1994).
[14] E. Saldin, V. Schneidmuller, and M. Yurkov, Opt. Commun. **97**, 272 (1993).
[15] L. Warstki *et al.*, J. Appl. Phys. **46**, 3644 (1975).
[16] C. E. Clayton *et al.*, Phys. Rev. Lett. **70**, 37 (1993).
[17] D. Umstadter, J. K. Kim, and E. Dodd, Phys. Rev. Lett. **76**, 2073 (1996).